

Thin film CdSe/CuSe photovoltaic on a flexible single walled carbon nanotube substrate[†]

Cite this: *Phys. Chem. Chem. Phys.*, 2013, **15**, 3930

Christopher E. Hamilton,^{†a} Dennis J. Flood^b and Andrew R. Barron^{*acd}

Liquid phase deposition (LPD), using CdSO₄ and *N,N*-dimethyl selenourea, has been used to grow CdSe absorber layer onto single walled carbon nanotube (SWNT) derived back contact substrates. The nanotubes are imbedded in, and penetrate into, the CdSe absorber layer for the goal of enhancing excitation dissociation and carrier transport. The Cd : Se film stoichiometry varied between 1 : 1.7 to 1 : 1.3 depending on the deposition conditions. The CdSe/SWNT layers show appropriate photoresponse. LPD was also used to grow a CuSe window layer onto which silver contacts were deposited. The resulting PV device shows a characteristic *I/V* curve. Despite both the open circuit voltage (V_{OC} = 1.28 mV) and short circuit current (I_{SC} = 4.85 μ A) being low, the resulting device is suggestive of the possibility of fabricating a flexible thin film (inorganic) solar cell by solution processes.

Received 21st November 2012,
Accepted 31st January 2013

DOI: 10.1039/c3cp50435b

www.rsc.org/pccp

1. Introduction

Solar generation of electricity has been an active area of research since shortly after Becquerel first discovered the photoelectric effect in 1839.¹ Concerns over fossil fuel production as well as issues of pollution and climate change have spurred intensive research into photovoltaics (PV) as well as other renewable energy sources. Solar is the most utilized of the 'green' energy sources to date. However, it has stalled with regard to market penetration. Given that the total solar energy adsorbed by the Earth is *ca.* 1×10^{22} J per day, which is enough to meet the world's energy needs for a year, sunlight is not a limitation of adoption. At present the main barrier to mass adoption is the cost in comparison with hydrocarbon and coal, in particular the increasing abundance of cheap natural gas. Thus, the only barriers to meeting global energy needs by PV technology are economic; *i.e.*, improvements in efficiency and reduction in manufacturing costs will be needed to reach grid-parity (when the per-watt cost of PV energy equals that of coal and natural gas).

While thin film solar cells still do not meet the efficiencies of single-crystal silicon cells, they are less expensive to manufacture, and the future viability of solar energy depends on advances in thin-film technology.² Still, many advances are required to reach grid-parity; a major goal is the reduction of solar cell cost to below 1 dollar per watt. The majority of thin film solar cells using cadmium telluride or copper-indium-gallium-selenide (CIGS) are produced using chemical vapour deposition (CVD) or other semiconductor manufacturing methods; these methods are energy-intensive and require specialized equipment. New methods will be required to produce inexpensive flexible thin film solar cells.

One of the problems associated with any compound semiconductor solar cell is that in order to have sufficient photon collection it is necessary to have a relatively thick absorber layer (Fig. 1a). However, a thick absorber layer will mean that there is a large diffusion length to the back contact, which results in a higher percentage of hole electron recombination, and hence lower efficiency. To overcome both these issues it would be desirable to design an absorber layer that has the back contact embedded within the layer (Fig. 1b). This would allow for a thick absorber layer, but a relatively short diffusion length. This will, in theory, allow for enhanced exciton dissociation and carrier transport.

Single walled carbon nanotubes (SWNTs) have a host of desirable physical and electronic properties that make them potential as conduction channels and back contact materials. In particular, metallic SWNTs are capable of ballistic electron transport on micron length scales, meaning they conduct electrical current with zero energy loss from scattering.³ In addition, their

^a Department of Chemistry, Rice University, Houston, TX 77005, USA.

E-mail: arb@rice.edu; Tel: +1 713 348 5610

^b Natcore Technology, Inc., 87 Maple Avenue, Red Bank, NJ 07701, USA

^c Department of Mechanical Engineering and Materials Science, Rice University, Houston, TX 77005, USA

^d College of Engineering, Swansea University, Singleton Park, Swansea SA2 8PP, Wales, UK. E-mail: A.R.Barron@swansea.ac.uk

[†] Electronic supplementary information (ESI) available: Photographic images of samples, PV testing configuration, and full fabrication scheme. See DOI: 10.1039/c3cp50435b

^{*} Present address: Materials Science & Technology Division, Los Alamos National Laboratory, MS E549, PO Box 1663, Los Alamos, NM 87545, USA.

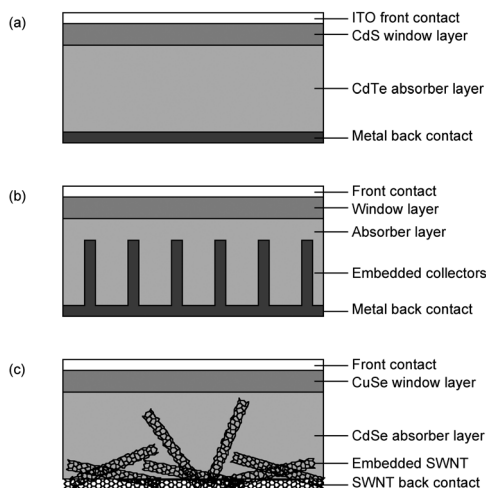


Fig. 1 Schematic diagram of (a) traditional thin film (CdTe) solar cell, (b) a thin film solar cell in which the back contact is embedded into the absorber layer, and (c) a potential SWNT-based thin film PV device.

high surface area ($\text{ca. } 1600 \text{ m}^2 \text{ g}^{-1}$)⁴ and their electron-accepting properties, mean that SWNTs have potential as both a conductive network in general, and as promoters of excitation dissociation. In fact, for these reasons carbon nanotubes in general have been investigated as a base extraction layer⁵ or hole transport layers⁶ in organic solar cells. Therefore SWNTs are an ideal candidate for use in PV applications; in fact they are currently being studied for use in transparent electrodes⁷ as well as in the active layer of organic photovoltaic (OPV) devices.⁸ SWNTs are mechanically flexible,⁹ allowing them to be deposited onto flexible substrates by filtration, spraying, or printing, providing an electrically conductive matrix onto which semiconductor films can then be deposited, creating an embedded conduction pathway within an absorber layer (Fig. 1c). The easiest method for creating a SWNT suitable for growth of a thin film is in the form of so-called Buckypaper.^{10,11} Commonly prepared by filtration of SWNT suspensions,¹² it has already been used in fuel cell and capacitor applications.¹³

A promising route to inexpensive PV devices is liquid phase deposition (LPD) also known as chemical bath deposition (CBD).^{14,15} This solution phase method allows the deposition of a variety of semiconductor thin films under ambient conditions using simple equipment found in any wet chemistry laboratory.¹⁶ LPD is well suited to the preparation of conformal films on flexible substrates, such as Buckypaper. Raffaele and co-workers have shown that CdSe quantum dots can be attached to SWNTs and used in polymer solar cells as a route to exciton dissociation and carrier transport.¹⁷ By contrast, previous research in our group focused on deposition of (12–16) semiconductor materials (CdS and CdSe) onto SWNTs in surfactant solutions.¹⁸ This study showed that uniform cadmium chalcogenide films could be prepared on SWNTs. Herein we demonstrate LPD preparation of cadmium and copper selenide films on preformed SWNT films, often called Buckypapers.

Cadmium selenide films deposited by LPD are n-type with a direct bandgap of 1.74 eV, while copper selenide LPD films are

p-type with a bandgap of 2.26 eV. SWNT PV devices described here, using cadmium selenide as the absorber material and copper selenide as the top (window) layer, could have, theoretically, efficiencies approaching 20%.¹⁹ The architecture of our proposed devices consists of Buckypaper at the back of the cell, covered and infiltrated with CdSe, which extends in a continuous layer above the SWNTs. Coating the CdSe with a layer of CuSe forms a bulk-heterojunction (Fig. 1c). The goal of this present study is to determine whether such a device architecture offer potential. The results of these initial experiments are presented herein.

2. Experimental

Deionized water was degassed prior to use by bubbling with argon for 15 minutes. CdSO_4 , $\text{CuSO}_4 \cdot 5\text{H}_2\text{O}$, NH_4OH (28–30%), Na_2SO_3 , sodium citrate, sodium dodecyl sulphate (SDS, $\text{Na}[\text{C}_{12}\text{H}_{25}\text{SO}_4]$), and elemental selenium were purchased from Sigma Aldrich and were used as received. *N,N*-Dimethyl selenourea [DMSU , $\text{Se}=\text{C}(\text{NH}_2)\text{NMe}_2$] was purchased from 3B Scientific Corp. Single-walled carbon nanotubes (HiPco process) were obtained from the Carbon Nanotube Laboratory at Rice University, and were purified following the literature procedure prior to use.²⁰

Stabilized DMSU solution was prepared by dissolving sodium sulfite (13 mg, 0.10 mmol) in deoxygenated, deionized water (10 mL). *N,N*-Dimethyl selenourea (151 mg, 1.0 mmol) was then added to the sulphite solution with stirring under argon. DMSU solutions decompose within 1–2 days even if stored under argon. Sodium selenosulphate solution was prepared by dissolving sodium sulphite (5.04 g, 0.04 mol) in deionized, deoxygenated water (100 mL). Selenium powder (1.58 g, 0.02 mol) was then added, and the mixture was heated to 60 °C with stirring for 2 h under argon. After 2 hours, residual Se was removed by filtration. Selenosulphate concentration is estimated at $\text{ca. } 0.18 \text{ M}$.²¹ Solutions are usable for 3–4 days if stored under argon.

XPS data were acquired on a Physical Electronics, Inc. Phi Quantera instrument with monochromated Al-K α X-ray source. SEM imaging was performed with a FEI Quanta 400 high-resolution field emission scanning electron microscope (accelerating voltage of 30 kV) equipped with liquid N_2 -cooled EDS detector. XRD data were acquired using a Rigaku D/Max Ultima II configured with a vertical theta/theta goniometer, Cu-K α radiation, and graphite monochromator. Raman data were obtained using a Renishaw Raman microscope with a 514 nm laser excitation source. Conductivity data were found using a four-point probe at a current of 0.5 mA. The photoconductance of the CdSe/Buckypaper and the Photoresponse of the CuSe/CdSe/Buckypaper samples were tested using literature protocols.²²

A schematic representation of the device fabrication steps is shown in Fig. 2. It should be noted that it is important for the SWNTs to only be imbedded into the lower CdSe absorber layer. If SWNTs remain uncoated prior to deposition of the CuSe window layer the cell will be short-circuited.

2.1. Buckypaper substrates

Buckypaper was prepared by a variation of literature methods.^{10,12} SWNTs (10 mg) were dispersed in 1% SDS solution (100 mL) and

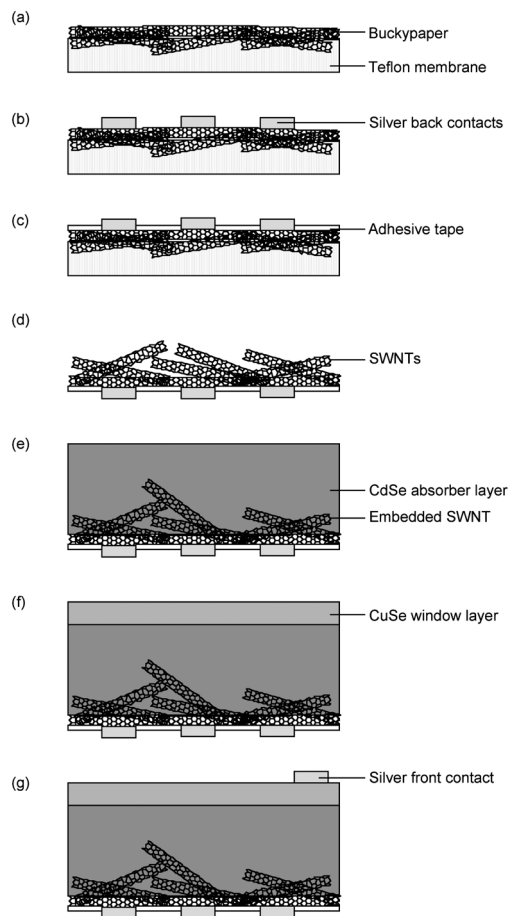


Fig. 2 Schematic representation of the fabrication steps employed: (a) deposition of SWNTs onto a Teflon membrane, (b) painting silver paste contacts, (c) attachment of adhesive tape to mask one side of the Buckypaper with alignment to the silver contacts, (d) removal of the Teflon membrane, (e) LPD growth of CdSe, (f) LPD growth of CuSe, and (g) painting silver paste contacts.

subjected to probe sonication for 60 minutes. The resulting SWNT dispersion (40 mL) was vacuum filtered over a PTFE membrane (47 mm diameter, 0.2 μm pore size), *i.e.*, Fig. 2a. After all solvent had been removed, conductive silver paint was brushed onto an area at the centre of the Buckypaper (Fig. 2b). The vacuum was left on for 2 minutes in order to allow silver to partially infiltrate the SWNTs. The paper was then inverted and pressed onto a piece of polyester packing tape (3M PET), which had been perforated with several holes by a needle in a small area (Fig. 2c). Care was taken to ensure that the silver paint was matched to the perforated area of the tape to allow electrical contact to be made from the back of the assembled 'Buckypaper-on-tape'. Before film deposition, the perforations in the tape were coated with a thin layer of rubber cement (Elmer's) to protect the back contacts from bath solutions.

2.2. CdSe deposition

To a glass jar was added CdSO_4 (6.0 mL, 0.10 M), sodium citrate (3.0 mL, 0.60 M), NH_4OH (2.4 mL, 1.50 M), deionized water (3.4 mL), and freshly prepared stabilized DMSU solution

(5.2 mL, 0.10 M). Moist substrates (immersed in water 5 minutes before drip drying) were immersed vertically in order to minimize bulk precipitate on their surfaces. The jar was capped and the reaction was allowed to proceed for 4 hours at room temperature. When the deposition was complete, samples were removed from the bath and rinsed with deionized water, then placed in a vacuum desiccator to dry.

2.3. CuSe deposition

To a glass jar was added CuSO_4 (5.0 mL, 0.20 M), NH_4OH (3.0 mL, 1.50 M), deionized water (7.0 mL), and Na_2SeSO_3 (5.0 mL, *ca.* 0.18 M). Moist substrates (immersed in water 5 minutes before drip drying) were immersed, vertically in order to minimize bulk precipitate on the surfaces. The jar was capped and the reaction was allowed to proceed for 16 hours at room temperature. When the deposition was complete, samples were removed from the bath and rinsed with deionized water, then placed in a vacuum desiccator to dry.

3. Results and discussion

Buckypaper substrates were prepared by simple vacuum filtration of SWNT dispersions through PTFE membranes. Buckypapers prepared from *o*-dichlorobenzene (ODCB) SWNT dispersions were found to have poor conductivity (*ca.* 400 S cm^{-1}). Films of adequate conductivity are obtained only after high temperature vacuum annealing. Several aqueous dispersions of SWNTs using various surfactants were then examined. Buckypapers produced from sodium dodecyl sulphate (SDS), sodium dodecylbenzenesulphonate (SDBS), and dodecyltrimethylammonium bromide (DTAB) showed conductivities of 1500, 500, and 800 S cm^{-1} , respectively. It should be noted that conductivity is dependent on film thickness, however, SEM showed all samples to have thicknesses of 2–3 μm . SDS is known to effectively suspend carbon nanotubes²³ and is the most commonly used surfactant for SWNTs. We have attributed the improved conductivity of Buckypapers cast from SDS to be as a consequence of a more homogeneous starting dispersion. Fig. 3 shows a typical Buckypaper deposited from SDS solution.

A general scheme for LPD of CdSe films involves the hydrolysis of *N,N*-dimethyl selenourea (DMSU) in alkaline conditions in the presence of a cadmium salt. A complexing ligand is also required in order to prevent precipitation of $\text{Cd}(\text{OH})_2$ as well as to regulate the concentration of free Cd^{2+} ions in solution.¹⁶ Typical complexing agents are sodium citrate or tartrate, triethanolamine, ethylenediamine, or nitrilotriacetic acid. Although on its face LPD appears to be a very simple process, in fact it is quite complex as a number of equilibrium and reactions are involved. Small changes in reaction conditions can have dramatic effects on the quality and properties of produced films.

LPD of most II–VI semiconductor films, including CdSe, is considered to occur by either of two possible mechanisms: ion-by-ion or hydroxide cluster. Eqn (1) gives the ion-by-ion mechanism. Similarly, the hydroxide cluster mechanism is described by eqn (2) and (3). For both mechanisms, the

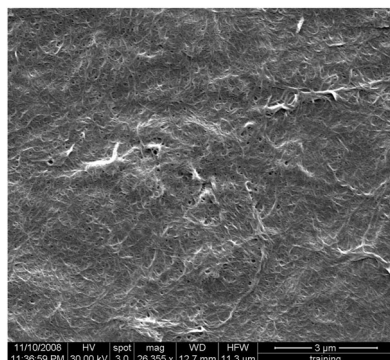
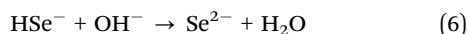
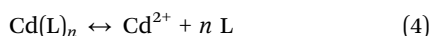
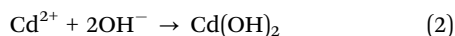


Fig. 3 SEM of Buckypaper prepared by filtration of SDS SWNT dispersion.

concentrations of Cd^{2+} and Se^{2-} are controlled by the reactions shown in eqn (4)–(6).



It is difficult to determine which mechanism is dominant for a given film deposition. In fact, both are operative to some degree under most reaction conditions.¹⁶ There are some conditions that favour one mechanism *versus* the other. In general, the hydroxide cluster mechanism can be favoured by increasing pH or by decreasing the ratio of ligand to cadmium. Increasing pH accelerates the formation of hydroxide clusters (by increased OH^- concentration); reducing the amount of complexant does the same by increasing available free Cd^{2+} . Usually the ion-by-ion mechanism gives slower depositions, but produced films have larger terminal thicknesses.¹⁶ Also, whether due to deposition rate or other factors, ion-by-ion films commonly have larger crystallites.

3.1. Deposition of CdSe absorber layer

CdSe films were deposited on Buckypaper from CdSO_4 and sodium sulphite-stabilized DMSU, using sodium citrate as the Cd complexing ligand, in aqueous ammonia solution (pH 10.4) at room temperature.^{21,24} Under these conditions it is expected that the hydroxide cluster mechanism is dominant. Films deposited onto SDS-derived Buckypapers on PTFE membranes (12 h deposition time) were shown by SEM to have incomplete infill of the void space between SWNTs. In addition, large numbers of colloidal CdSe particles were present on the films' surfaces (Fig. 4a). Since the production of an efficient PV device depends critically on the quality of the p–n heterojunction, a planar interface is desired, free from defects or debris. Furthermore, if cracks in the CdSe layer expose SWNT to subsequent deposition of the CuSe layer, and hence will result in a short circuit of the device. Reduction of the reagent concentrations

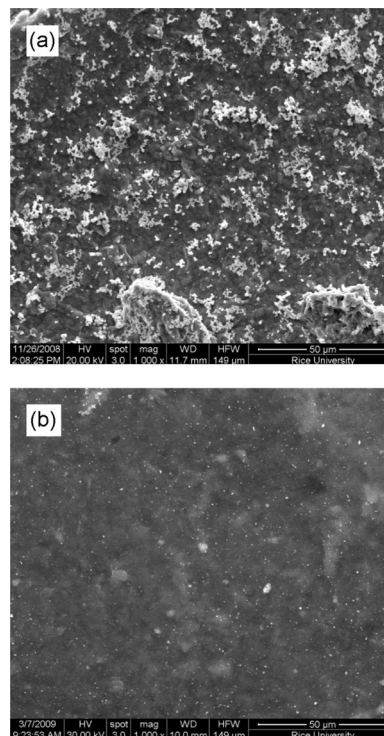


Fig. 4 SEM images of CdSe films on Buckypaper: deposition times were 12 h (a) and 4×4 h (b).

had no effect on improving the quality of the films; in fact when the bath concentration is reduced the deposition rate on the substrate is retarded with no concomitant slowing of bulk precipitation (*i.e.*, thinner films, same colloidal debris). Performing multiple 4 h depositions from fresh baths produced uniform films with clean surfaces although complete infill required 16 total hours (Fig. 4b).

X-ray photoelectron spectroscopy (XPS) analysis showed the stoichiometry of the films produced to contain an excess of cadmium, having Cd : Se ratios of between 1.7 : 1 and 1.9 : 1. Energy-dispersive X-ray spectroscopy (EDS) confirmed the XPS data. Further analysis showed a large amount of oxygen present. It is understood that oxygen chemisorbs to metal chalcogenide films;²³ moreover, known impurities in LPD films include cadmium hydroxides and cadmium carbonates.²⁵ The presence of these impurities explains the imbalance between cadmium and selenium. Degassed water was subsequently used to prepare all solutions and resulted in films of negligible oxygen content.

The stoichiometry of CdSe films produced with degassed water was found by EDS to be selenium rich; Cd : Se ratios were *ca.* 1 : 1.7. The disparity is attributed to the formation of zero valent selenium, which precipitates from solution as a black or red solid and likely becomes entrapped in the film. Lower concentrations of selenium relative to cadmium only resulted in slowed deposition and had no effect on film composition.

The ratio of stabilizer to selenium was varied as a second experiment. Sodium sulphite is a reducing agent used to slow the oxidation of DMSU and prevent the formation of bulk selenium. Increasing the ratio of sulphite : Se from 1 : 10 to

Table 1 Effect of citrate : cadmium ratio on deposited CdSe film stoichiometry (as determined by EDS)

Citrate : cadmium ratio	Cd : Se film stoichiometry
4.0 : 1	1 : 1.7
3.5 : 1	1 : 1.4
3.0 : 1	1 : 1.2
2.5 : 1	1 : 1.3
2.0 : 1	No film

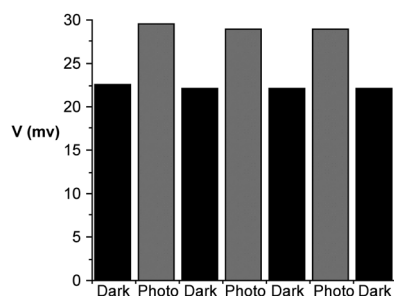
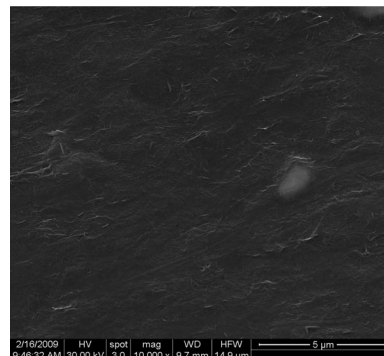
1.5 : 10 had no effect on film composition. Conversely, as hydrolysis of DMSU is believed to be the rate-limiting step for LPD of CdSe films,¹⁶ the sulphite : Se ratio was also lowered to 1 : 20. It was thought that this would increase the deposition rate, resulting in better CdSe films. Unfortunately this approach failed; deposited films were even higher in selenium.

Finally, the ratio of citrate to cadmium was lowered; the rationale being that increased concentrations of $\text{Cd}(\text{OH})_2$ (assuming hydroxide cluster mechanism) or free Cd^{2+} (ion-by-ion) should consume Se^{2-} before it can be oxidized to Se^0 . Ratios were varied between 2 : 1 and 4 : 1. For citrate : Cd ratios below 3 : 1, visible $\text{Cd}(\text{OH})_2$ formed immediately on addition of ammonia, and below 2.5 : 1 film deposition was poor. Changing this parameter did effectively alter film stoichiometry (Table 1). A citrate to cadmium ratio of 3 : 1 produces films containing minimal excess selenium.

The photoconductivity of The CdSe film was tested prior to cell fabrication (Fig. S1, ESI†). This allows for the rapid screening of materials or synthesis variable of a single material even before issues of cell design and construction are considered. The voltage was measured with a shutter held over the sample and with the shutter removed. The difference in voltage is a direct indication of the change in the photo-conductance of the sample. As may be seen from Fig. 5 there is a distinct photo-response for the CdSe.

3.2. Fabrication of back contacts

Attempts to perform electrical tests on the CdSe films on Buckypaper/PTFE were hampered by difficulty gaining electrical contact to the back surface of the SWNTs. Several remedies were attempted, including sputtering of gold onto the back of the Buckypaper after peeling it from the Teflon membrane or using conductive silver adhesive. Very thin Buckypaper substrates are

**Fig. 5** Photoresponse of a Buckypaper coated with LPD grown CdSe.**Fig. 6** SEM image of 'Buckypaper-on-tape' (SWNT side).

too fragile to be removed from the backing membranes, so a different solution was needed.

By painting the top surface of the Buckypaper with conductive silver adhesive while it is under suction in a filtration apparatus, it is possible to partially impregnate silver within the SWNT network (Fig. 2a and b). Care must be taken, however, not to use too much silver or to leave the vacuum on too long. If silver bleeds through to the underside of the SWNTs, clean separation of the Buckypaper from the Teflon membrane is not possible.

After the silver paint dried the Buckypaper was inverted and carefully transferred to the adhesive side of a strip of PET packing tape (Fig. 2c). The tape had been perforated in a small area, corresponding to the position of the silver on SWNTs. Next the filter membrane was carefully peeled away, transferring the SWNTs to the adhesive tape (Fig. 2d and Fig. S2, ESI†). Before subjecting the Buckypaper to LPD, holes in the packing tape were masked by rubber cement to prevent CdSe from depositing on the back contacts. Resulting Buckypapers have a very smooth top surface as seen by SEM (Fig. 6). In addition they are flexible, robust and do not delaminate from the tape, even under the conditions of LPD.

3.3. Second-generation CdSe Buckypaper

Deposition of CdSe on Buckypaper-on-tape (Fig. 2e), using the conditions optimized above, yielded surprising results. After 16 hours of deposition (4×4 h), SEM imaging revealed that the films were severely cracked (Fig. 7). SEM further showed that the films were much thicker than those from previous Buckypaper samples. One explanation for this observation could be that Buckypaper-on-packing tape samples have a smoother top surface that allows rapid nucleation and therefore faster film growth. Alternately, it is possible that SWNTs on tape are of higher density at the deposition surface since they have been inverted (and also compressed with sufficient force to adhere them to the tape), and therefore less time or material is required to infill the void space.

The observed extensive cracking is problematic, as any direct contact of SWNTs to the window layer will short the heterojunction. Cracking could be attributed to excessive flexing of the substrate, either during LPD or subsequent SEM sample preparation. Thick films are likely to be more brittle,

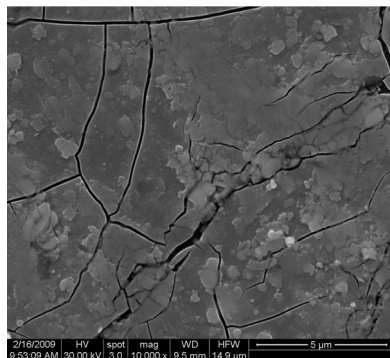


Fig. 7 SEM image of CdSe (16 h deposition) on Buckypaper-on-tape.

compounding the formation of cracks. In order to learn whether sample handling was causing film cracking, a small piece of Buckypaper-on-tape was affixed to an aluminium SEM sample stub. The stub was coated with rubber cement to protect it from the LPD solution, and then CdSe was deposited on the immobilized Buckypaper. SEM revealed, again, a large amount of cracking of the CdSe film. Therefore, cracking is not (at least not entirely) caused by samples flexing during handling. It is still unclear whether the problem is due to internal stresses within the film or some other factor.

To overcome this problem shorter depositions were studied on Buckypaper-on-tape samples. Severe cracking occurs after 12 h of deposition. At 4 and 8 hours, uniform films with smooth top surfaces are formed (Fig. 8 and Fig. S3, ESI[†]). While some cracks are still visible in SEM, they are much fewer and smaller.

XRD was attempted on CdSe SWNT composites; however the samples did not diffract. Either the material is truly amorphous, or the crystalline domains are smaller than *ca.* 4 nm. However, previous XRD studies of similar LPD CdSe films deposited on glass required annealing before any weak diffraction was observed.²¹

3.4. Deposition of CuSe window layer

CuSe window layer was deposited on top of the CdSe layer (Fig. 2f). However, initial attempts to deposit copper selenide using DMSU and citrate at 60 °C were not reproducible; the films were inconsistent in both thickness and quality. All previous CuSe LPD methods using DMSU have resulted in films

of the klockmannite phase (CuSe).^{26,27} The desired phase for PV window layers is berzelianite (Cu_{2-x}Se, where *x* ≈ 0.2), as it has better conductivity. Therefore, an alternate selenium source was examined, sodium selenosulfate (Na₂SeSO₃). Na₂SeSO₃ is conveniently prepared by heating elemental selenium in an aqueous solution of sodium sulphite. It is unstable (though less so than DMSU) and must be kept from oxygen to avoid bulk precipitation of elemental Se.

Several selenosulphate CuSe preparations were attempted, using citrate²⁶ or NTA¹⁶ as copper complexants. Also tested were reaction schemes employing only NH₃ as ligand.^{28,29} The method of Garcia *et al.*²¹ provided the best quality films. SEM images of the CuSe films show colloidal material and small crystallites on the surface (Fig. 8).

Determination of CuSe film composition and thickness on CdSe Buckypapers was nontrivial. Equivalent films (16 h deposition) grown on glass have a thickness of 200 nm.²⁶ EDS data was collected to find average film stoichiometry. The presence of a small amount of cadmium (3%) was detected. EDS sampling depth is on the order of 1 μm; the presence of trace cadmium implies that CuSe films are in fact approximately 1 μm thick.

Analysis by XPS also showed the presence of cadmium (*ca.* 2%). Since XPS is a surface technique, this close agreement between XPS and EDS was confusing. It was assumed that Cd in EDS resulted from the underlying absorber layer; cadmium was not expected to be present at the surface. Taken together, XPS and EDS suggested that either CuSe films are doped with small amounts of cadmium, or that CuSe coverage is incomplete. SEM images taken over large areas showed uniformity of the surface texture; thus the films appear to be homogeneous (Fig. 9).

Further information was obtained by XPS depth profiling. Iterative ion sputtering and elemental analysis showed cadmium present only at the surface of the film. Upon sputtering into the sample cadmium content disappears completely (as does oxygen), leaving a consistent stoichiometry of Cu_{1.7}Se throughout the film. It was not possible to sputter through the CuSe window layer down into the CdSe absorber. Finally, based upon XPS and EDS, it appears the CuSe window layer is of the desired berzelianite stoichiometry, has a thickness of *ca.* 1 μm, and is contaminated at the surface by cadmium.

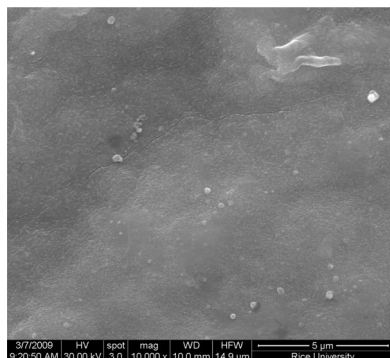


Fig. 8 SEM image of CdSe film (4 h deposition) on Buckypaper-on-tape.

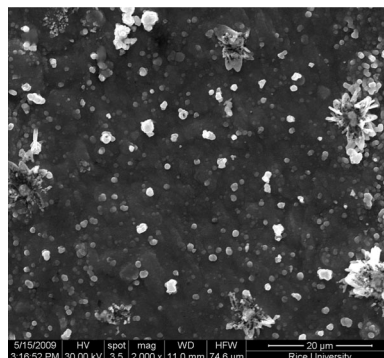


Fig. 9 SEM image of CuSe film on CdSe on Buckypaper-on-tape.

The presence of cadmium at the sample surface is most likely due to cadmium species (hydroxides, carbonates) previously adsorbed on the surface of the CdSe film are re-dissolved in the CuSe LPD bath and then subsequently re-deposited onto the CuSe window layer. Another explanation is that metals are significantly mobile within the films. In fact, this has been shown previously: CdSe films have been doped with copper by simple immersion in aqueous Cu^{2+} solutions.²⁹ Additionally, in CdS films cadmium can be exchanged with copper *quantitatively* down to a depth of 300 nm by an aqueous bath method.³⁰ However, these explanations would be expected to result in small amounts of Cd throughout the film or close to the CuSe/CdSe interface, not at the top surface. Whatever the source of the cadmium, it is not expected to have a significant effect on the function of PV devices.

XRD was performed in order to determine the phase of CuSe present. The film has some crystallinity, as weak diffraction was seen with peaks matching bulk berzelianite Cu_{2-x}Se , further corroborating XPS data (Fig. 10).

As a final characterization, depth-profile Raman spectra were collected on the films. CuSe and CdSe have their strongest Raman modes at 263 and 209 cm^{-1} respectively. It must be mentioned that these frequencies are coincident with the radial breathing modes (RBMs) of SWNTs found between 150 and 250 cm^{-1} . Thus, care must be taken when assigning peaks. Additionally, Raman depth profile data suffers from limitations. Scattering occurs from above and below the focal plane, therefore depth slices overlap. Also, deeper slices suffer from reduced signal to noise due to significant scattering from the sample above the focal plane.

Raman spectra were collected with the microscope focal plane varied from 2 μm above the sample surface to 2 μm below in 1 μm steps. The resulting spectra show none of the expected peaks attributable to SWNTs (D, G modes) and contain a single (CuSe) peak at 263 cm^{-1} . Spectra collected with the focal plane at the surface and 1 μm below show a very slight peak begin to appear at 209 cm^{-1} , indicating CdSe (Fig. 11). Unfortunately, at 2 μm depth and below, baseline noise increased so that no peaks were observed. Scattering expected for SWNTs was not seen in any spectrum, indicating that the semiconductor coatings are microns thick.

3.5. PV testing

Devices were subjected to testing for photovoltaic response. It should be noted that the devices described here have not yet

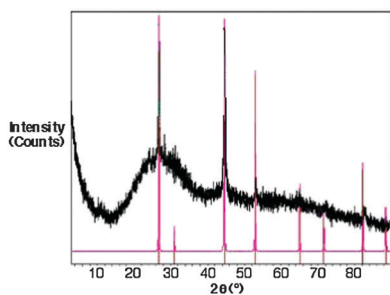


Fig. 10 XRD pattern of CuSe–CdSe Bucky paper. The simulated pattern for berzelianite (JCPDS Card No. 06-0680) is shown.

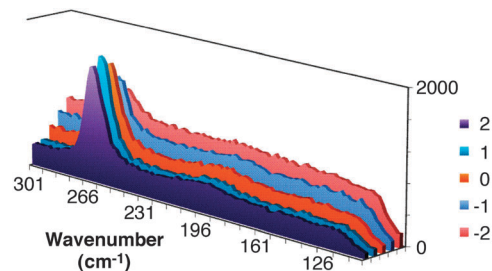


Fig. 11 Depth-profile Raman spectra (514 nm excitation) of CuSe–CdSe Bucky paper, from +2 to −2 μm relative to sample surface.

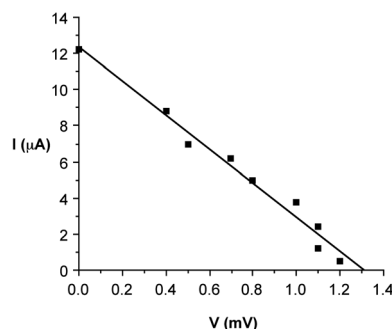


Fig. 12 Characteristic I – V curve for test device ($R^2 = 0.985$).

been optimized in terms of relative or absolute film thickness of the metal selenides. Additionally, as-prepared devices lack a transparent top contact. For testing purposes, silver adhesive paint was adequate to provide proof of concept (Fig. 2g). Fig. S5 (ESI†) shows the testing configuration. The goal of this test was to determine if the concept is viable rather than create a working device.

Device testing was performed (top contact: silver paint spots) which confirmed PV functionality, albeit with minimal efficiency. The characteristic IV curve for the test device is shown below (Fig. 12). The open circuit voltage (V_{OC}) was found to be 1.28 mV; short circuit current (I_{SC}) was 4.85 μA . For a device to be viable, V_{OC} will need to be increased by nearly 3 orders of magnitude; likewise short-circuit current should be in the mA range. Nevertheless, we believe that given the un-optimised nature of the device with regard to film thickness, top and bottom contacts, and the film doping levels as defined by the composition, the ability to create a active device through simple LPD processing offers hope that inorganic thin film devices can be prepared through simple chemical processes.

4. Conclusions

We have demonstrated a functional, albeit highly inefficient, thin film solar cell produced by a LPD method, which can be manufactured on flexible substrates. Many improvements are still needed in terms of design, performance, and production. In particular, further characterization of semiconductor films is needed to find optimal thickness and to improve crystallinity.

However, our work provides proof-of-concept and suggests that the architecture and method of production offer promise. We note that recently, the use of carbon nanotube carpets have shown promise with CdTe/CdS solar cell;³¹ however, the CdTe layers was on top of the nanotube arrays and there was minimal inter-penetration.

No attempt was made in this study to optimize the doping of the semiconductor layers. In future it will be important to ensure that the LPD grown layers are uniform in composition and doping. In addition, it should be noted that as prepared the SWNT samples contain approximately 15–20% metallic tubes, the remainder being semiconducting. This will contribute to the lower that desired conductivity and hence charge separation.

Another task yet to be completed is the design of a transparent top contact that will not increase manufacturing costs. Conductive material is required, in order to collect charge carriers across the entirety of the top surface. The top contact must also be optically transparent so that light reaches the absorber layer. Materials suitable for our device include poly(3,4-ethylenedioxythiophene)–poly(styrenesulfonate) (PEDOT:PSS) and transparent conductive oxides (TCOs) such as ITO or fluoride-doped tin oxide. Other potential materials are SWNT or graphene polymer composites.

Acknowledgements

This work was supported by the Robert A. Welch Foundation (C-0002).

Notes and references

- H. J. Moller, *Semiconductors for Solar Cells*, Artech House, Boston, 1993.
- M. Pagliaro, G. Palmisano and R. Ciriminna, *Flexible Solar Cells*, Wiley-VCH, Weinheim, 2008.
- P. J. F. Harris, *Carbon Nanotubes and Related Structures*, Cambridge University Press, Cambridge, 1999.
- B. J. Landi, R. P. Raffaele, S. L. Castro and S. G. Bailey, *Prog. Photovolt.: Res. Appl.*, 2005, **13**, 165.
- S. Cataldo, P. Salice, E. Menna and B. Pignataro, *Energy Environ. Sci.*, 2012, **5**, 5919.
- E. Kymakis, M. M. Stylianakis, G. D. Spyropoulos, E. Stratakis, E. Koudoumas and C. Fotakis, *Sol. Energy Mater. Sol. Cells*, 2012, **96**, 298.
- S. De, P. E. Lyons, S. Sorel, E. M. Doherty, P. J. King, W. J. Blau, P. N. Nirmalraj, J. J. Boland, V. Scardaci, J. Joimel and J. N. Coleman, *ACS Nano*, 2009, **3**, 714; G. Fanchini, S. Miller, B. B. Parekh and M. Chhowalla, *Nano Lett.*, 2008, **8**, 2176; A. A. Green and M. C. Hersam, *Nano Lett.*, 2008, **8**, 1417.
- V. Sgobba and D. M. Guldi, *J. Mater. Chem.*, 2008, **18**, 153; D. M. Guldi, G. M. A. Rahman, F. Zerbetto and M. Prato, *Acc. Chem. Res.*, 2005, **38**, 871; D. M. Guldi, G. M. A. Rahman, N. Jux, N. Tagmatarchis and M. Prato, *Angew. Chem., Int. Ed.*, 2004, **43**, 5526; S. Roy, R. Bajpai, A. K. Jena, P. Kumar, N. Kulshrestha and D. S. Misra, *Energy Environ. Sci.*, 2012, **5**, 7001; N. J. Alley, K.-S. Liao, E. Andreoli, S. Dias, E. P. Dillon, A. W. Orbaek, A. R. Barron, H. J. Byrne and S. A. Curran, *Synth. Met.*, 2012, **162**, 95.
- M. W. Rowell, M. A. Topinka, M. D. McGehee, H. J. Prall, G. Dennler, N. S. Sariciftci, L. B. Hu and G. Gruner, *Appl. Phys. Lett.*, 2006, **88**, 233506.
- E. T. Mickelson, C. B. Huffman, A. G. Rinxler, R. E. Smalley, R. H. Hauge and J. L. Margrave, *Chem. Phys. Lett.*, 1998, **296**, 188.
- J. L. Delgado, M. Á. Herranz and N. Martín, *J. Mater. Chem.*, 2008, **18**, 1417.
- A. Mazzoldi, D. De Rossi and R. H. Baughman, *Proc. SPIE*, 2000, **3987**, 25; U. Vohrer, I. Kolaric, M. H. Haque, S. Roth and U. Detlaff-Weglikowska, *Carbon*, 2004, **42**, 1159; L. J. Sweetman, L. Nghiem, I. Chironi, G. Triani, M. in het Panhuis and S. F. Ralph, *J. Mater. Chem.*, 2012, **22**, 13800.
- Z. Niu, W. Zhou, J. Chen, G. Feng, H. Li, W. Ma, J. Li, H. Dong, Y. Ren, D. Zhao and S. Xie, *Energy Environ. Sci.*, 2011, **4**, 1440.
- P. J. Sebastian and P. K. Nair, *Adv. Mater. Opt. Electron.*, 1992, **1**, 211; P. J. Sebastian, A. Sanchez and P. K. Nair, *Adv. Mater. Opt. Electron.*, 1993, **2**, 133; P. J. Sebastian and H. Hu, *Adv. Mater. Opt. Electron.*, 1994, **4**, 407; P. J. Sebastian, H. Hu and A. M. Fernández, *Adv. Mater. Opt. Electron.*, 1995, **5**, 11.
- T. Rattanaavoravipa, T. Sagawa and S. Yoshikawa, *Sol. Energy Mater. Sol. Cells*, 2008, **92**, 1445; C.-J. Huang, M.-P. Hwang, Y.-H. Wang and W.-J. Chang, *Jpn. J. Appl. Phys.*, 1998, **37**, L158; L. P. Deshmukh, P. P. Hankare and V. S. Sawant, *Sol. Cells*, 1991, **31**, 549.
- G. Hodes, *Chemical Solution Deposition of Semiconductor Films*, Marcel Dekker, New York, 2003.
- B. J. Landi, C. M. Evans, J. J. Worman, S. L. Castro, S. G. Bailey and R. P. Raffaele, *Mater. Lett.*, 2006, **60**, 3502; B. J. Landi, S. L. Castro, H. J. Ruf, C. M. Evans, S. G. Bailey and R. P. Raffaele, *Sol. Energy Mater. Sol. Cells*, 2005, **87**, 733.
- R. Loscutova and A. R. Barron, *J. Mater. Chem.*, 2005, **15**, 4346.
- J. Nelson, *The Physics of Solar Cells*, Imperial College Press, London, 2003.
- I. W. Chiang, B. E. Brinson, A. Y. Huang, P. A. Willis, M. J. Bronikowski, J. L. Margrave, R. E. Smalley and R. H. Hauge, *J. Phys. Chem. B*, 2001, **105**, 8297.
- V. M. Garcia, M. T. S. Nair, P. K. Nair and R. A. Zingaro, *Semicond. Sci. Technol.*, 1996, **11**, 427.
- D. J. Flood and A. R. Barron, A Simple Test Apparatus to Verify the Photoresponse of Experimental Photovoltaic Materials and Prototype Solar Cells, Connexions Web site. <http://cnx.org/content/m42271/1.3/>, Nov. 18, 2012.
- V. C. Moore, M. S. Strano, E. H. Haroz, R. H. Hauge, R. E. Smalley, J. Schmidt and Y. Talmon, *Nano Lett.*, 2003, **3**, 1379.
- M. T. S. Nair, P. K. Nair, H. M. K. K. Pathirana, R. A. Zingaro and E. A. Meyers, *J. Electrochem. Soc.*, 1993, **140**, 2987.
- A. Klyner, J. Lindgren and L. Stolt, *J. Electrochem. Soc.*, 1996, **143**, 2662.
- V. M. Garcia, P. K. Nair and M. T. S. Nair, *J. Cryst. Growth*, 1999, **203**, 113.

- 27 C. A. Estrada, P. K. Nair, M. T. S. Nair, R. A. Zingaro and E. A. Meyers, *J. Electrochem. Soc.*, 1994, **141**, 802.
- 28 M. Lakshimi, K. Bindu, S. Bini, K. P. Vijayakumar, C. Sudha Kartha, T. Abe and Y. Kashiwaba, *Thin Solid Films*, 2000, **370**, 89.
- 29 I. Grozdanov, C. K. Barlingay and S. K. Dey, *Integr. Ferroelectr.*, 1995, **6**, 205.
- 30 M. Savelli and J. Bougnot, Solar Energy Conversion, in *Topics in Applied Physics*, ed. B. O. Seraphin, Springer, Berlin, 1979, vol. 31, p. 213.
- 31 R. E. Camacho, A. R. Morgan, M. C. Flores, T. A. McLeod, V. S. Kumsomboone, B. J. Mordecai, R. Bhattacharjea, W. Tong, B. K. Wagner, J. D. Flicker, S. P. Turano and W. J. Ready, *JOM*, 2007, **59**, 39.